Future Projections of the East Australian wave climate.

Mark A. Hemer[1], K. L. McInnes[2] and R. Ranasinghe[3]

[1]. The Centre for Australian Weather and Climate Research (CAWCR): A partnership between CSIRO and the Bureau of Meteorology. CSIRO Marine and Atmospheric Research. Hobart, Tas. 700. Australia.
[2]. CAWCR, Aspendale, Vic. Australia.
[3]. UNESCO-IHE, and Technical University of Delft, The Netherlands.

1. Introduction

The most urbanised sector of the Australian coast is found along the eastern margin, and population within the coastal local government areas in these regions has shown significantly greater growth than the National growth rate over the past decade (Gurran et al., 2008). There is potential for communities and assets along the eastern coastline to increasingly come under threat from a range of climate change driven impacts. These include coastal flooding and erosion due to rising mean sea levels and possible changes in weather patterns which drive changes in wave climate and sea level extremes such as storm surges. Coastal erosion can occur in response to several factors. Increases in mean sea level, and the frequency and/or intensity of storms can increase the cross-shore transfer of sediment, while changes in wave direction in response to shifting storm patterns can alter the along-shore transfer of sediment, causing horizontal shifts in the shoreline position observed as erosion/accretion.

Sea level rise, and to a lesser degree the contribution of changing storm patterns to storm surges, has received an increased amount of attention along the Australian coast over recent years (Hardy et al, 2004, Church et al., 2006, McInnes et al., 2009). However to date only minimal consideration has been given to how the surface wave climate along the eastern Australian coast will vary under projected climate conditions (McInnes et al, 2007). The aim of this study is to provide more rigorous projections of the offshore ocean wave climate of the eastern Australian continental margin, to provide a suitable dataset which can be used to assess the possible coastal impacts of climate change in the region.

Waves observed along the eastern Australian coast are generated by a large range of meteorological systems: tropical cyclones, east-coast cyclones, mid-latitude cyclones, zonal anticyclonic highs and local summer seabreezes (Short and Treneman, 1992), which all drive wave events of similar magnitude, but have significantly different directional components. Swell waves generated in the Southern Ocean or in the central Pacific may also have some influence on the coast in the region. In order to resolve the complete spectrum of waves which are observed in this region, we have used a suite of 3rd generation spectral wave models, forced with downscaled, projected climate change scenarios. Recent studies investigating historical trends in the eastern Australian wave climate exhibit no significant change in

wave heights in the approximately 25 year historical record (Lord and Kulmar, 2000, Hemer et al., 2009), however strong relationships between wave direction and climatological forcing in the region, particularly associated with the ENSO cycle on interannual time-scales (Ranasinghe et al., 2004; Goodwin, 2005), the Interdecadal Pacific Oscillation on interdecadal time-scales (Goodwin, 2005), and at longer time-scales (Goodwin et al., 2006), have been reported.

2. Methodology

2.1 Regional downscaling of the Global climate change projections

Projections of future climate change include a range of uncertainties that require consideration in climate impacts research. An ensemble modelling approach is recommended, where model simulations using different models (multi-model ensembles) with different forcing conditions (perturbed physics ensembles) are used, under a range of emission scenarios which influence future atmospheric composition. The Coupled Model Intercomparison Project (Meehl et al., 2007) produces large numbers of runs from global climate models (GCM) which provide projections of future climate on a global scale. While most of these models provide relatively consistent projections of global mean parameters, results at a regional scale can be highly variable. This is attributed in part to the coarse resolution with which these models operate, which limits their ability to adequately resolve the regional flow patterns and to differences in the treatment of sub-grid scale processes. Wave models require suitable surface winds as forcing, and consequently it is important the regional wind patterns are well represented. The approach which is commonly adopted is to dynamically downscale results from the GCM's by nesting a limited area, high resolution regional atmospheric climate model (RCM), into a sub-domain of the GCM. As an alternative we use output from a variable resolution GCM (Conformal Cubic Atmospheric Model; CCAM, McGregor and Dix, 2008) acting as a RCM. This offers the advantage of avoiding lateral boundary reflections which can cause spurious results within the RCM (McGregor, 2005). This study uses the results of a number of CCAM model runs which have been carried out for the Climate Futures Tasmania (CFT) project (CFT, 2009), which dynamically downscales a number of GCM's from bias-adjusted sea-surface temperatures (SSTs) and sea-ice directly (i.e., no atmospheric forcings; Katzfey et al., 2009). CCAM is employed in a stretched mode, using the Schmidt (1977) transformation, which leads to a resolution of approximately 60km over the Australian region (Figure 1).

The 60km CFT CCAM runs were carried out to provide an ensemble of twelve climate change realisations, for the period 1960-2100. The bias-adjusted SSTs and sea-ice were obtained from six different GCMs (CSIRO Mk3.5, GFDLCM2.0, GFDLCM2.1, ECHAM4, MIROC and HADCM3) under two different emission scenarios (SRES A2 and SRES B1, representing high and low range emission scenarios, respectively). No perturbed physics ensembles are included within the run-set. In addition to these runs, CCAM was also used to dynamically downscale the NCEP/NCAR Re-analysis (NRA) onto the same grid, providing a dataset to compare the present climate. In this latter

run, the spectral nudging scheme described in Thatcher and McGregor (2009) was applied to fields of surface pressure and winds and temperatures at all model levels above 900 hPa,. This manuscript details future climate results from only a single set of runs (CSIRO Mk3.5, A2 Scenario). Results from the remaining wave model runs are not yet available.

The CFT CCAM model runs were carried out with the primary aim of projecting future terrestrial climate (temperature and precipitation variables), and further details of the skill of the models to represent the climate were presented by Grose (2009). The CFT project has only minor interest in the surface circulation over the ocean. We have taken the near-surface marine wind fields at 10-m height, archived at 6-hourly intervals, from three 20 year time-slices (1981-2000; 2031-2050; and 2081-2100) to force the wave model (see section 2.3). The wind fields are bi-linearly interpolated onto the 0.5 degree latitude-longitude grid on which the coarse resolution wave model is implemented.

2.2 Surface Wind bias adjustment

Surface winds derived from CCAM runs which dynamically downscale GCMs under present climate conditions are found to differ significantly from observed and re-analysis derived surface winds (see Section 3). We consider NRA surface winds are a suitable dataset for forcing a wave model in the region, based on prior wave modelling studies which provide adequate wave hindcasts using NRA winds (e.g., Swail et al., 1998). For a single climate run (e.g., CCAM CSIRO Mk3.5, A2 scenario), we therefore carry out two experiments: 1) un-corrected CCAM derived winds; and 2) bias-adjusted CCAM derived winds (to align with NRA winds) for all time-slices. The bias adjustment procedure used to correct the CCAM winds adjusts the joint probability distribution of eastward (u) and northward (v) wind components (to maintain directionality of the winds).

The joint-probability of the u and v wind components is determined for the 1980-2001 20-yr time slice for the CCAM winds, and for the 'observed' (NRA over the same period) winds for each model grid cell (at identical locations). We then seek to adjust the CCAM distribution for each location such that it more closely matches the observed distribution at that location. This is done by firstly distributing the zonal winds (u) into N percentile bands, and performing a standard distributed bias adjustment on the u-component winds. i.e., the xth percentile of CCAM u is adjusted to fit the xth percentile of the observed u. The u bias adjustment value is stored as a function of location, and the u percentile (i.e., an Nx1 matrix for each location). Then within each u percentile band of both datasets, the v-component winds are distributed into M percentile bands yielding an NxM matrix at each model grid point for the observed and the CCAM winds. The differences between the two matrices are calculated and used to adjust the CCAM wind percentiles. The matrix of bias adjustments is also used to adjust the CCAM future time-slices (i.e., the bias adjustment is assumed to be time invariable).

2.3 Wave Modelling

The response of the wave climate to projected climate change scenarios is investigated using a numerical wave model. The WaveWatch 3 (version 2.2; Tolman, 2002) was implemented at coarser resolution over the larger domain, with a nested finer resolution SWAN model (Booij et al., 1999, ,Ris et al., 1999) in the region of interest (Figure 2). The coarse grid, with a spatial resolution of 0.5° x 0.5° latitude-longitude grid c overs the domain 90°- 240°E, 65°- 0°S, spanning the Australia and South-West Pa cific region. The fine resolution grid, with a spatial resolution of 0.1° x 0.1° latitude-longitude grid covers the domain 150°- 155°E, 38°- 25°S, spannin g the region of interest along the coast of the state of New South Wales (NSW) in south eastern Australia. For both grids, wave spectra were calculated with a directional resolution of 15° and at 25 frequencies ranging non -linearly from 0.04 Hz to 0.5 Hz (corresponding to wave periods 25 s – 2 s). For the coarse grid, seasonally varying sea-ice conditions were based on monthly mean southern ocean ice concentrations derived from an 18-yr climatology (1973-1990) from the National Snow and Ice Data Center (Chapman and Walsh, 1996). The influence of variable ice conditions was considered to have only minor influence on the wave climate of the area of interest, and were assumed to remain constant for each time-slice (i.e., only the annual cycle of ice conditions were considered).

The wave models were initially run for a 5-yr period (1996-2000) using NRA 10-m wind forcing. Model parameters were tuned to optimise the fit of model integrated wave parameter outputs (primarily significant wave height, Hs, with some consideration of wave period, Tp and wave direction, Dp) with integrated wave parameters obtained from six waverider buoy records located along the NSW coast (Figure 2, Table1), and spatial comparisons of significant wave height outputs with altimeter derived wave height climatology presented by Hemer et al. (2009). The fit between wave parameters was initially optimised for the coarse resolution model (WaveWatch), and once the best fit was achieved for the coarse model, the fine resolution wave model (SWAN) parameters were tuned to achieve the best fit. WaveWatch outputs were primarily sensitive to two tunable parameters: STABSH (a wind scaling factor; Tolman, 2002) and SWELLF (a swell attenuation factor; Tolman, 2002). STABSH was varied between 0.9 and 1.65 (WaveWatch default 1.38), and SWELLF was varied between 0.02 and 1.0 (WaveWatch default 0.1), and the best fit was achieved with STABSH = 1.0 and SWELLF = 0.1. Outputs from the Nested SWAN model were sensitive to the choice of the whitecapping parameterisation. Significant improvement in the fit of wave period was achieved using the parameterisation described by Rogers et al (2002), which weights the relative wavenumber so that dissipation is reduced in low frequencies and increased in high frequencies. Further tuning of n, being the power of the relative wave number in the dissipation sink term (Equation 6, Rogers et al., 2002), was carried out in order to achieve the best comparison of wave height and period at the 6 buoy locations. The best fit was achieved with $n = 1.25$. To reduce run-time for the long time integration (20-years), a time-step of 3-hours is used within the SWAN model, requiring the use of the BSBT propagation scheme.

3. Results

3.1 Surface Winds

We assess the surface winds from the regionally downscaled models to address a number of objectives:
1) Do the un-bias-adjusted surface winds from the CCAM regional climate model adequately describe the present day wave climate?
2) Does the bias adjustment provide an adequate dataset to describe the seasonal variability of surface winds in the region under the present climate?
3) How much variability exists in the CCAM derived surface winds between the multi-model ensembles, in present-climate conditions and in projected time-slices?
4) How much variability exists in the CCAM derived surface winds between SRES scenarios?

In order to address these questions, the following surface wind datasets (over specified time-slices) are assessed below:
1. NRA (1981-2000)
2. CCAM downscaled NRA (RANL; 1981-2000)
3. CCAM Mk3.5 SRES A2 (1981-2000, 2031-2050, 2081-2100)
4. CCAM Mk3.5 SRES B2 (2031-2050, 2081-2100)
5. Bias Adjusted CCAM Mk3.5 SRES A2 (1981-2000, 2031-2050, 2081-2100)
6. CCAM GFDLcm2.0 SRES A2 (1981-2000, 2031-2050, 2081-2100)
7. CCAM GFDLcm2.1 SRES A2 (1981-2000, 2031-2050, 2081-2100)

3.1.1 Present-day climate surface winds

Figure 3 shows 20-yr (1981-2000) mean eastward and northward surface wind components along the 155°E meridian from each model (including NRA). The 10-year (Aug 1999- Jul 2009) mean QuikSCAT wind components are overlaid, assumed to represent the present day surface wind climate (i.e., assumed stationary over analysis period). QuikSCAT winds are obtained from the monthly IFREMER 0.5° gridded MWF (CERSAT, 2002) . There is little variability between the CCAM runs, despite the different parent GCMs used to force the regional model. All of the CCAM runs nudged with GCM forcing overestimate the zonal wind speeds when compared to NRA and QuikSCAT winds. The bias corrected CCAM Mk3.5 winds are seen to overlay the NRA winds exactly. Mean NRA winds are observed to differ considerably from the QuikSCAT winds. A portion of this difference can be attributed to the different time periods over which the means are determined, however the dominant portion of this difference is ascribed to the misrepresentation of the surface circulation in this region by the NRA.

Figure 4 shows the 20-yr (1981-2000) standard deviation of the eastward and northward wind components along the 155°E meridian from each model (including NRA). The standard deviation of the QuikSCAT surface wind components is not shown, as the number of observations is much fewer. Although generally similar to each other in magnitude, the CCAM model

simulations underestimate the zonal wind standard deviation by about 1 ms^{-1} between 45-55°S and overestimate it by about 0.5 ms^{-1} at around 40°S. The meridional wind in the CCAM simulations is larger by about 0.5 ms^{-1} south of 25°S.

Figure 5 demonstrates the effectiveness of the CCAM model to represent the seasonal variability. The bias-adjusted CCAM Mk3.5 surface winds display seasonal variability of similar magnitude to the NCEP model, despite the bias adjustment being independent of time.

3.1.2 Projected climate surface winds

Figure 6 shows the 20-yr mean eastward and northward wind components from each CCAM model, for three time-slices (1981-2000, 2031-2050 and 2081-2100), along the 155°E meridian. The future ti me-slices are taken from the SRES A2 scenario. The dominant zonal component, displays little variation between models, or temporal change. The meridional component of the surface wind shows greater temporal change, with meridional surface wind speeds decreasing by approximately 1ms^{-1} (increasing southward component) across all latitudes in the 2081-2100 time-slice. Little variation is observed between models south of 35°S. North of thi s latitude, CCAM GFDLCM2.1 projects less temporal change than the other two models.

Only minor differences are observed between the two scenarios assessed (SRES A2 and SRES B1). In the meridional wind component (which displays the major component of temporal change under projected conditions), the low range SRES B1 scenario has mean meridional winds projected to decrease in magnitude by approximately 70-80% of the decrease projected for the high range SRES A2 scenario (not shown). No significant differences are observed in the zonal component.

Figure 6 also illustrates that the the projected temporal change in surface winds under the SRES scenarios A2 (and B1) is smaller than the bias correction which was applied to the CCAM Mk3.5 surface winds to align them with NRA conditions. Similarly, the variation between the present climate CCAM runs (Mk3.5, GFDLCM2.0 and GFDLCM2.1) is smaller than the bias correction. Therefore, for the analysis of wave model results in the following sections, we have concentrated on the CCAM Mk3.5 and bias-adjusted CCAM Mk3.5 (Mk3.5-BA) datasets, which display a greater variation of surface wind forcing, than the multi-model, or emission scenario ensembles.

Nevertheless, it should be noted that since the following wave model results are based on only a single ensemble member, an assessment of the uncertainty in the future wave conditions represented by this model cannot be made.

3.2 Wave Model Results

We focus on the results of seven wave model 20-yr time-slice runs. These include three present-day climate (1981-2000) time-slices (NCEP forced,

CCAM Mk3.5 forced, and Bias Adjusted CCAM Mk3.5 forced); two SRES A2 scenario mid-century (2031-2050) time-slices (CCAM Mk3.5 forced, and Bias Adjusted CCAM Mk3.5 forced); and two SRES A2 scenario end-of-century (2081-2100) time-slices (CCAM Mk3.5 forced, and Bias Adjusted CCAM Mk3.5 forced). These runs are used to:

      1) determine whether the CCAM wind forcing is suitable for describing the present day wave climate, and in particular to determine whether the outlined bias adjustment procedure improves the model; and

      2) use the projected conditions to describe one potential future climate scenario for the east Australian wave climate.

3.2.1 Present-day wave climate

The skill of the wave model is assessed using climatological comparisons of integrated wave parameters (Hs, Tp, Tm and Dp) from the model, with those from the NSW waverider buoys. To test whether two distributions are co-aligned, we use the chi-squared statistic (Wilks, 2006):

$$\chi^2 = \sum_{i=1}^{n} \frac{\left(O_i - E_i\right)^2}{E_i}$$

Where O_i is the observed frequency for the i-th bin (from model), E_i is the expected frequency for the i-th bin (from observations). n is the number of bins in the PDF. When determining χ^2 for the directional values, to ensure that each level of the categorical variable had an expected frequency count of at least 5%, χ^2 was determined over the range of 60 to 180° (with 15° bins, i.e., 9 bins). Smaller χ^2 values indicate a better fit to the expected distribution, The probability associated with the χ^2 test statistic was determined from the chi-square cumulative distribution function. The p-value was determined, dependent on the degrees of freedom (df = n-1).

Figure 7a overlays the modelled significant wave height distributions from the three present climate time-slice (1981-2000) wave model runs at the location of the Sydney waverider buoy, with distributions derived from the Sydney waverider buoy and the NOAA WW3 model, which was found to be the best performing model for the Australian region by Hemer et al. (2007). Figures 7b and 7c display equivalent results for integrated parameters Tp and Dp respectively. Table 2 summarises the fit of each model for each parameter at all locations. The bias adjustment of the surface winds improves the model fit of wave height at 5 of the 6 locations. The CCAM Mk3.5-BA model shows considerable improvement in the wave height distributions over the NWW3 model. In comparison to the un-adjusted data, the bias adjustment to the surface winds improves the fit of peak wave period to observations at 4 of the 6 sites, but improves the fit of peak wave direction at just 1 of 3 locations. Output from the Mk3.5-BA model displays a closer fit than the NWW3 model to observations for all wave parameters. The chi-squared goodness of fit tests indicate that the models are only able to reproduce the observed distribution of significant wave height within 95% confidence intervals. None of the models are able to simulate the observed distribution of wave period or direction.

Comparisons of wave period between the CCAM forced models and observations show that the wave model underpredicts the peak wave period, missing a large proportion of the long swell period (>10s) waves. This is consistent with the wave direction results (Fig 7c), which show a decreased proportion of southerly waves (associated with the longer wave periods) and an increased proportion of the north-easterly waves (associated with shorter wave periods). There are two possible causes for these results: 1) in-sufficient waves being generated in the southern ocean propagating to the NSW coast, or 2) too much dissipation of swell energy. Further investigation of prior tuning runs display no improvement with varied parameters, and work is continuing to improve the fit of the modelled wave period. Transfer to WaveWatch3 version 3.14 (Tolman, 2009) is underway to update model physics, and to also make use of the mosaic grid approach, removing the dependence on two model codes (i.e., Remove nested SWAN).

Figure 8 shows the mean annual cycle of integrated wave parameters at the location of the Sydney waverider buoy. Comparisons of the Hs mean annual cycle show that the smallest root-mean-square error is recorded for Run CCAM Mk3.5-BA from the selection of present climate runs. Consistent with the results of Short and Treneman (1992), there is minimal variability in the annual cycle of Hs. The underestimation of the peak wave period is observed to be consistent all year. Modelled wave directions display greater seasonal variability than observed. Observed and modelled wave directions compare well during the Austral winter months, but during the summer months, the mean direction has less of a southerly component than the observations, suggesting that the decreased proportion of southerly events occurs primarily during the summer months.

3.2.2 Projected wave climate changes

Figure 9 displays projected changes in the bivariate Hs vs Dp distribution at the Sydney waverider buoy location, from the CCAM Mk3.5-BA run (SRES A2 scenario), showing the difference between the mean 1981-2000 and 2081-2100 distributions. Qualitatively, we see a projected decrease in Hs, brought about by a decrease in the upper tail of the distribution, and a shift in wave direction from a wave climate dominated by southerly wave events, to one that is dominated by north-easterly wave events. Large southerly wave events are replaced by north-easterly events with significant wave height near to the mean value. Little change in wave period is projected (not shown).

Table 3 summarises the projections of mean wave climate at each of the buoy sites for the SRES A2 scenario. Results from the unadjusted CCAM Mk3.5 run are also shown, to demonstrate that the bias-adjustment procedure does not alter the qualitative nature of the projected changes in the wave climate. A decrease in mean Hs is observed at 5 of the 6 locations, and wave direction shows a shift to a greater easterly component at all sites. Projected changes in wave period are less clear.

Projected changes, as a function of month of year (Figure 10) indicate mean Hs projections show a greater decrease in months May to July (Austral winter months). Directional changes are greater during months Aug-Sep (Winter to Spring). This suggests that the differences are driven by changes in the systems which drive wave events during this period (e.g., mid-latitude cyclones, which are the major cause of south-easterlies along the Sydney coast, Short and Treneman, 1992). The observed changes suggest decreasing influence of these systems, which would be consistent with a southward shift in the position of the southern ocean storm belt, as projected to occur with the increasing positive polarity of the Southern Annular Mode in a projected warmer climate with increasing greenhouse gases (Cai et al., 2003).

The projected changes in wave height are most pronounced in the upper tail of the wave height distribution. Projected shifts in the behaviour of extreme events (defined as those which exceed a 3 m threshold) are shown in Table 4 for both CCAM Mk3.5 and CCAM Mk3.5-BA model sets. The behaviour of extreme events is described by the frequency, duration and intensity of the events exceeding a 3 m threshold. We see a decreasing frequency of extreme events, but observe no significant changes in the duration or intensity of these events.

4. Discussion & Concluding Remarks

We make use of surface wind datasets available from a dynamical downscaling project, where the CCAM model has been used to downscale six GCM's (CSIRO Mk3.5, GFDLcm2.0, GFDLcm2.1, ECHAM4, MIROC and HADCM3) for two SRES scenarios (the high and low end scenarios, A2 and B1 respectively). Assessment of the marine surface winds in the Tasman Sea from three of these runs (CSIRO Mk3.5, GFDLcm2.0 and 2.1) indicate relatively small variability amongst this subset of the multi-model ensembles. We also find relatively small variability between emission scenarios for the downscaled CSIRO Mk3.5 runs. The variability between climate model ensembles is small relative to the adjustment applied to the surface winds. The joint-probability distributed bias adjustment is applied to the CCAM derived surface winds to correct the winds to a more realistic wind field for the region (as defined by the NRA surface winds), and enable the direction and magnitude distribution to be consistent with the NRA winds.

Corrected and un-corrected winds from the CCAM downscaled CSIRO Mk3.5, A2 scenario run have been used to force a suite of spectral wave models to provide projections of wave climate along the east Australian coast under a warmer climate scenario.

Model skill was assessed by comparing integrated wave parameters derived from the model with those from six waverider buoys along the NSW coast. For present climate conditions, a JPD bias-adjustment procedure applied to the surface winds was shown to improve the skill of the wave model. The model outperforms NWW3 in the region across all integrated wave parameters. The model predicts the observed distribution of significant wave

height within 95% confidence limits. Improvements are underway to improve model period and directional performance. The ability of the model to reproduce the Hs distribution allows confidence in the models ability to represent projected changes in surface winds from the RCM on projected Hs. Greater uncertainty exists in the projection directional changes.

Wave climate projections from the downscaled CSIRO Mk3.5 A2 scenario winds indicate a decrease in mean significant wave height, which is likely to be associated with a decrease in frequency of the large southerly wave events. This leads to a shift in the mean wave direction, such that the dominant wave direction which is south-easterly in present climate conditions shifts to be north-easterly under the projected warmer climate scenario.

The projected wave climate results presented here provides only one realisation of future wave climate conditions. Analysis of wave model results derived from a larger range of climate model simulations of future wind conditions is needed to assess the uncertainty surrounding the future wave climate changes presented here.   Effort will be made to reduce this uncertainty with ongoing work. The wave modelling procedure will be repeated for an increased number of the available downscaled climate model ensembles and emission scenarios. The project aims to determine an ensemble mean projected wave climate from three models (CSIRO Mk3.5, GFDLcm2.0 and GFDLcm2.1), for two scenarios (A2 and B1).

References

Booij et al., 1999 N. Booij, R.C. Ris and L.H. Holthuijsen, A third generation wave model for coastal regions. Part 1: model description and validation, *J. Geophys. Res.* **104** (C4) (1999), pp. 7649–7666.

Cai W.J., P.H. Whetton and D.J. Karoly. 2003. The response of the Antarctic Oscillation to increasing and stabilised CO2. *Journal of Climate* 16, 1525–1538.

CFT, 2009. Climate Futures for Tasmania.
http://www.acecrc.org.au/drawpage.cgi?pid=climate_futures [Accessed 29-Sep-2009].

Chapman, W.L., and J.E. Walsh. (1996). *Arctic and Southern Ocean sea ice concentrations*. Boulder, CO: National Snow and Ice Data Center/World Data Center for Glaciology. Digital media.

Church, J.A., J.R. Hunter, K.M. McInnes and N.J. White, 2006. Sea-level rise around the Australian coastline and the changing frequency of extreme sea-level events. *Australian Meteorological Magazine*, 55, 253-260.

Goodwin, I.D., 2005. A mid-shelf wave direction climatology for south-eastern Australia, and its relationship to the El Niño – Southern Oscillation since 1877 AD, *Int. J. Climatol.* 25, 1715–1729

Goodwin, I.D., M.A. Stables and J.M. Olley, 2006. Wave climate, sand budget and shoreline alignment evolution of the Iluka-Woody Bay sand barrier, northern New South Wales, Australia, since 3000yr BP. *Marine Geology*, 226(1-2), 127-144.

Grose, M. 2009. Climate variability and change in Tasmania over the twentieth century as a framework for examining climate. *Book of abstracts: 9th International Conference on Southern Hemisphere Meteorology and Oceanography. 9-13 Feb 2009*, Melbourne Australia.

Gurran, N., E. Hamin and B. Norman, 2008. Planning for climate change: Leading practice principles and models for sea change communities in coastal Australia. *Report prepared for the National Sea Change Taskforce. July 2008.* Available at:
http://www.seachangetaskforce.org.au/Publications/PlanningforClimateChange.pdf [Accessed 28-Sep-2009].

Hardy, T., L. Mason, A. Astorquia and B. Harper 2004: Queensland climate change and community vulnerability to tropical cyclones: Ocean hazards assessment. Report to Queensland Government. 45pp + 7 appendices
http://www.longpaddock.qld.gov.au/ClimateChanges/pub/OceanHazards/Stage2LowRes.pdf

Hemer, M.A., J.A Church and J.R. Hunter, 2007. Waves and climate change on the Australian coast. *J. Coastal Res.,* SI50, 432-437.

Hemer, M.A., J.A Church and J.R. Hunter, 2009. Variability and trends of the directional wave climate of the Southern Hemisphere. *International Journal of Climatology*, In Press.

CERSAT (2002) Quikscat scatterometer mean wind field products use manual. Available at: ftp://ftp.ifremer.fr/ifremer/cersat/products/gridded/mwf-quikscat/documentation/mutwqscat.pdf. [Accessed: 29-Sep-2009].

Katzfey, J.J., J. McGregor, K. Nguyen and M. Thatcher, 2009. Dynamical downscaling techniques: Impacts on regional climate change signals. *Proceedings of the 18th World IMACS / MODSIM Congress, Cairns, Australia 13017 July 2009.* 3942-3947.

Lord, D., and M. Kulmar, 2000. The 1974 storms revisited: 25 years experience in ocean wave measurement along the south-east Australian coast. In: B.L. Edge (Ed), *Proceedings of the 27th International Conference on Coastal Engineering. ASCE, Sydney, Australia.* 559-572.

McGregor, J. L., 2005. C-CAM: Geometric aspects and dynamical formulation. CSIRO Marine and Atmospheric Research Technical Report 70. http://www.cmar.csiro.au/e-print/open/mcgregor_2005a.pdf

McGregor, J. L., and Dix, M. R., 2008. An updated description of the conformal-cubic atmospheric model. High Resolution Simulation of the Atmosphere and Ocean, Hamilton, K. and Ohfuchi, W., Eds., Springer, 51-76

McInnes, K.L., Macadam, I., Hubbert, G.D. and O'Grady, J.G. 2009: A Modelling Approach for Estimating the Frequency of Sea Level Extremes and the Impact of Climate Change in Southeast Australia. *Natural Hazards* 51 115–137. DOI 10.1007/s11069-009-9383-2.

McInnes, K. L., I. Macadam, D. Abbs, S. P. O'Farrell, J. O'Grady, and R. Ranasinghe. 2007. Projected changes in climatological forcing conditions for coastal erosion in NSW. *Proceedings of Coasts and Ports '07, Melbourne, VIC, Australia. On CD Rom produced by Engineers Australia*

Meehl, G.A., C. Covey, T. Delworth, M. Latif, B. McAvaney, J.F.B. Mitchell, R.J. Stouffer, and K.E. Taylor, 2007. The WCRP CMIP3 Multimodel Dataset: A New Era in Climate Change Research *Bull. Amer. Meteor. Soc.*, **88**, 1383-1394.

Ranasinghe, R., R. McLoughlin, A. Short and G. Symonds. 2004. The Southern Oscillation Index, Wave Climate, and Beach Rotation. *Marine Geology*, Vol. 204, 273-287

Ris et al., 1999 R.C. Ris, L.H. Holthuijsen and N. Booij, A third-generation wave model for coastal regions. 2. Verification, *J. Geophys. Res.* **104** (C4) (1999), pp. 7667–7681.

Rogers, W.E., P.A Hwang and D.W. Wang. 2002. Investigation of wave growth and decay in the SWAN model: Three regional scale applications. *J. Phys. Oceanog.,* 33(2), 366-389.

Schmidt, F., 1977. Variable fine mesh in spectral global models. Beitr. Phys. Atmos., 50, 211-217.

Short, A.D. and N.L.Treneman (1992) Wave climate of the Sydney region, an energetic and highly variable ocean wave regime. *Aust. J. Mar. Freshwater Res.* 43, 765-791.

Swail, V.R., V.J. Cardone and A.T. Cox, 1998. A long term North Atlantic wave hindcast. Fifth International Workshop on Wave Hindcasting and Forecasting. January 26-30, 1998. Melbourne, Florida.

Tolman, H. 2002: User manual and system documentation of WAVEWATCH-III version 2.22. NOAA / NWS / NCEP / MMAB Technical Note **222**, 133 pp. [Available at: http://polar.ncep.noaa.gov/mmab/papers/tn222/MMAB_222.pdf]

Tolman, H. 2009: User manual and system documentation of WAVEWATCH III™ version 3.14. NOAA / NWS / NCEP / MMAB Technical Note **276**, 194 pp + Appendices. [Available at:
http://polar.ncep.noaa.gov/mmab/papers/tn276/MMAB_276.pdf]

Thatcher, M and J. L. McGregor, 2009: Using a scale-selective filter for dynamical downscaling with the Conformal Cubic Atmospheric Model. *Mon. Weath. Rev.* **137,** 1742-1752**.**

Wilks, D.S., 2006. Statistical methods in the Atmospheric Sciences. *Academic Press,* 627pp.

Tables

Table 1. Summary of buoys used for model validation. Data obtained from the Manly Hydraulics Laboratory. NSW State Govt. A 20-yr mean is determined where possible, regardless of dates.
[1] Denotes directional waverider buoy
[2] Sydney waverider was directional from 03-Mar-1992

Site Name	Latitude (°S)	Longitude (°E)	Water Depth	Date of first obs	Date of final obs
Byron Bay[1]	28.82	153.73	71	01-Jan-1981	31-Dec-2000
Coffs Harbour	30.36	153.27	72	01-Jan-1981	31-Dec-2000
Crowdy Head	31.83	152.86	79	01-Jan-1986	31-Dec-2005
Sydney[1,2]	33.78	151.44	85	01-Jan-1988	31-Dec-2005
Port Kembla	34.47	151.03	78	01-Jan-1981	31-Dec-2000
Batemans Bay[1]	35.71	150.34	73	01-Jan-1987	31-Dec-2005

Table 2. Summary statistics of the fit of modelled distribution of integrated wave parameters for present climate runs (1981-2000) against distribution obtained from waverider buoy records. The period of coverage of the buoy data varies by buoy (see Table1), but assumed representative of present climate. Bold text indicates best fit (defined by smallest χ^2 value). An asterisk denotes that the modelled distribution fits the observed distribution (with 95% confidence ($p<0.05$), according to a chi-squared goodness of fit test.

χ^2	Mk3.5	Mk3.5-BA	NCEP	NWW3
Hs: Byron	9.55	**2.00***	2.24*	7.05
Coffs	9.84	5.07	**0.72***	17.8
Crowdy	18.8	1.81*	**1.07***	12.6
Sydney	9.73	**1.15***	1.87*	6.09*
Pkembla	2.53*	**1.87***	6.37	6.40
Batemans	**3.36***	9.79	12.8	57.3
Tp: Byron	37.9	**30.9**	34.5	36.6
Coffs	36.8	28.6	**25.6**	39.3
Crowdy	34.0	31.2	**29.1**	50.7
Sydney	52.9	51.0	**47.2**	82.9
Pkembla	38.4	44.6	**37.2**	51.2
Batemans	**25.7**	32.3	32.1	95.4
Dp: Byron	20.5	17.1	**14.9**	53.0
Coffs	-	-	-	-
Crowdy	-	-	-	-
Sydney	34.8	42.2	**24.7**	79.2
Pkembla	-	-	-	-
Batemans	**44.5**	67.6	71.1	258.7

Table 3. Mean wave climate projections at NSW buoy sites. The asterisks denote consistent trends across the three time-slices. Significant wave height (Hs) has units of metres; Peak wave period has units of seconds; Peak wave direction has units of degrees clockwise from North.

Variable/Location	1981-2000		2031-2050		2081-2100	
	Mk3.5	Mk3.5-BA	Mk3.5	Mk3.5-BA	Mk3.5	Mk3.5-BA
Hs: Byron	1.79	1.71	1.75	1.64	1.68*	1.58*
Coffs	1.72	1.72	1.68	1.65	1.63*	1.61*
Crowdy	1.90	1.70	1.84	1.63	1.78*	1.59*
Sydney	1.80	1.67	1.74	1.58	1.71*	1.56*
Pkembla	1.66	1.64	1.59	1.56	1.58*	1.55*
Batemans	1.52	1.27	1.46	1.20	1.46	1.21
Tp: Byron	8.43	8.45	8.34	8.29	8.24*	8.26*
Coffs	8.50	8.42	8.41	8.27	8.31*	8.20*
Crowdy	8.64	8.52	8.59	8.36	8.51*	8.30*
Sydney	8.37	8.17	8.35	8.02	8.31*	8.02
Pkembla	8.36	7.98	8.34	7.82	8.29*	7.83
Batemans	8.55	8.07	8.56	7.95	8.52	7.92*
Dp: Byron	123.0	132.0	118.4	130.7	115.4*	124.8*
Coffs	120.3	131.8	116.1	130.4	112.4*	125.2*
Crowdy	127.7	134.4	124.7	131.7	120.4*	126.4*
Sydney	119.9	130.2	116.0	127.3	111.9*	122.8*
Pkembla	111.4	123.5	107.9	120.5	104.0*	116.1*
Batemans	105.3	115.1	102.0	111.9	98.9*	107.6*

Table 4. 90th percentile wave climate projections at NSW buoy sites. Period and Direction are mean of values greater than 90th percentile threshold. ExF is exceedance frequency (events per year) over threshold of 3.0m (translates to approx 98th percentile). The asterisks denote consistent trends across the three time-slices. Significant wave height (Hs) has units of metres; Peak wave period has units of seconds; Peak wave direction has units of degrees clockwise from North; Mean Event Duration (mD) has units of hours; Mean Intensity (mI) of event has units of metres over the 3 m threshold.

Variable/Location	1981-2000		2031-2050		2081-2100	
	Mk3.5	Mk3.5-BA	Mk3.5	Mk3.5-BA	Mk3.5	Mk3.5-BA
Hs: Byron	2.66	2.63	2.57	2.53	2.45*	2.44*
Coffs	2.52	2.70	2.42	2.60	2.31*	2.47*
Crowdy	2.89	2.68	2.74	2.53	2.61*	2.43*
Sydney	2.77	2.63	2.63	2.47	2.57*	2.42*
Pkembla	2.52	2.59	2.40	2.44	2.36*	2.42*
Batemans	2.29	1.99	2.17	1.85	2.15*	1.85
Tp: Byron	9.64	9.74	9.50	9.64	9.38*	9.58*
Coffs	10.0	10.04	9.80	9.87	9.62*	9.76*
Crowdy	10.30	10.51	10.08	10.34	9.89*	10.13*
Sydney	9.70	9.92	9.47	9.69	9.32*	9.56*
Pkembla	9.59	9.50	9.41	9.30	9.27*	9.21*
Batemans	9.57	9.72	9.42	9.51	9.29*	9.41*
Dp: Byron	147.2	149.3	142.3	143.8	142.5	141.6*
Coffs	148.2	159.2	142.8	155.1	142.8	151.6*
Crowdy	163.0	155.5	161.6	154.7	163.4	152.8*
Sydney	149.4	148.4	147.9	147.5	147.1*	142.8*
Pkembla	134.0	138.3	130.3	138.8	129.5*	134.6
Batemans	109.7	114.2	104.8	115.2	106.5	114.8
ExF: Byron	17.2	23.3	15.2	20.4	12.2*	16.9*
Coffs	14.5	24.6	12.05	23.2	9.1*	18.4*
Crowdy	28.4	24.1	24.2	20.2	20.1*	17.3*
Sydney	28.3	25.0	26.0	20.5	22.6*	18.0*
Pkembla	18.7	26.1	14.5	21.2	14.7	21.6
Batemans	9.9	5.85	6.7	3.46	6.3*	3.54
mD: Byron	28.3	21.7	28.4	21.3	24.5	19.8*
Coffs	26.1	23.7	24.2	21.8	24.3	21.6*
Crowdy	27.2	23.8	25.1	23.6	24.6*	22.2*
Sydney	23.2	21.5	19.5	21.2	20.6	21.8
Pkembla	22.5	19.5	20.7	19.1	19.2*	18.5*
Batemans	24.4	20.7	23.5	26.7	20.9*	23.9
mI: Byron	0.65	0.65	0.61	0.61	0.58*	0.60*
Coffs	0.57	0.80	0.50	0.69	0.53*	0.73
Crowdy	0.80	0.86	0.73	0.79	0.73	0.80
Sydney	0.89	0.88	0.72	0.81	0.77	0.83
Pkembla	0.73	0.86	0.61	0.82	0.56*	0.80*
Batemans	0.67	0.56	0.54	0.54	0.50*	0.47*

Figures
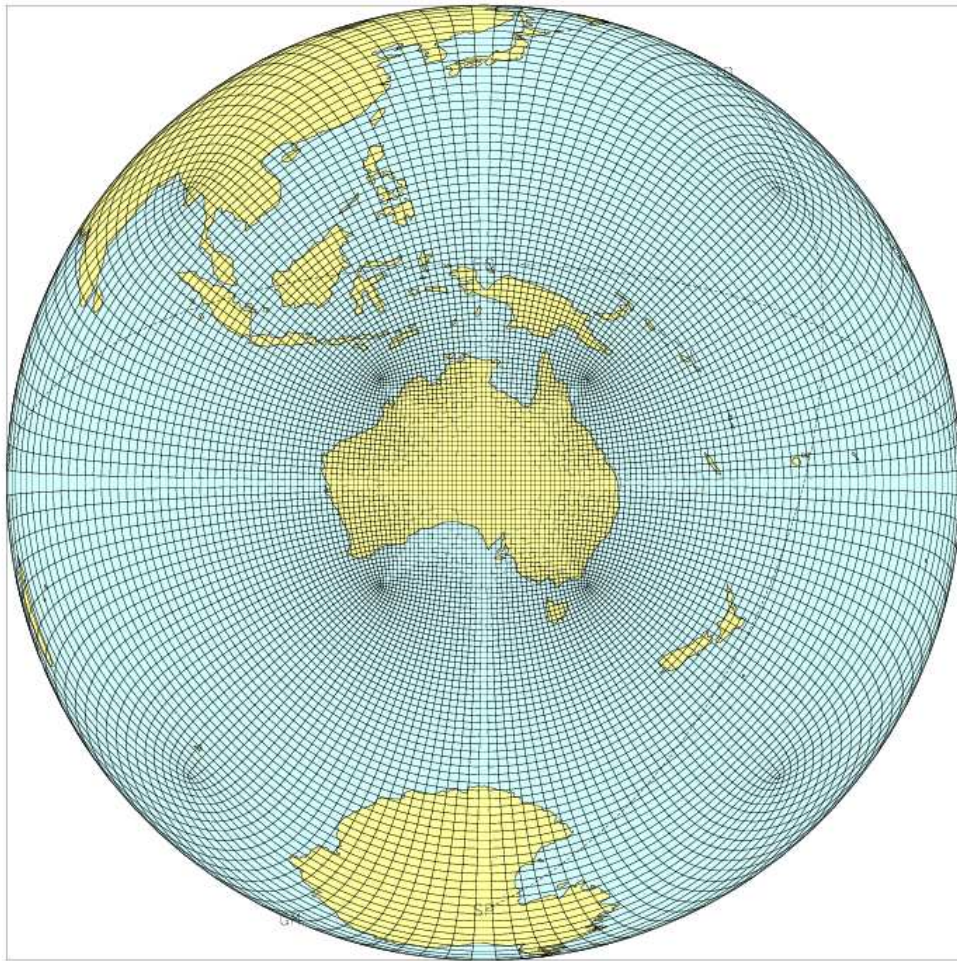
Figure 1. A view of the CCAM C64 grid, having a resolution over the Australian region of approximately 60km.

a)

b)
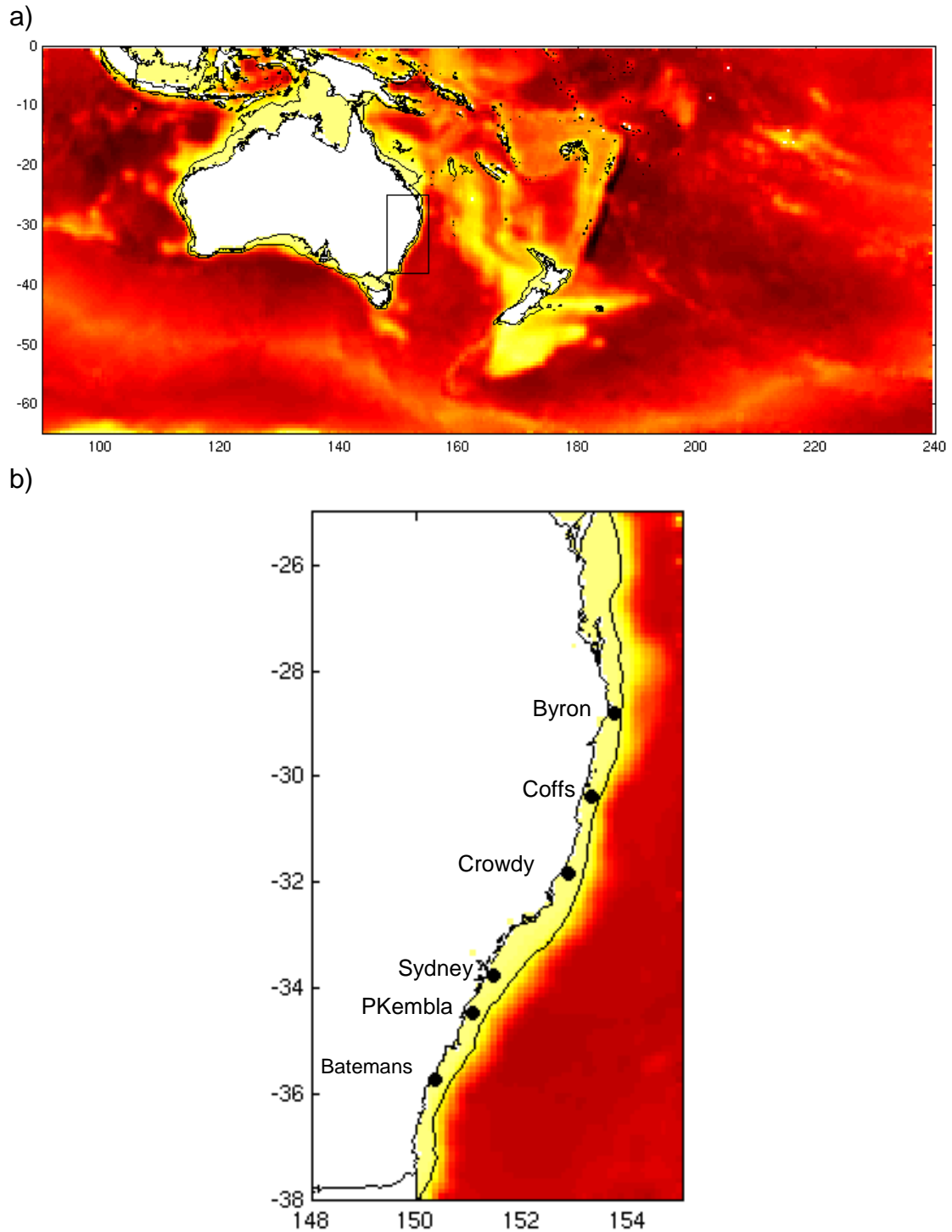
Figure 2. Wave Model grids with 200-m depth contour shown. a) 0.5°
resolution WaveWatch 3 domain. Box shows nested SWAN model domain, as
shown in more detail in plot b). b) 0.1° resolution nested SWAN domain.
Western boundary is at 150°E. Black dots indicate location of waverider buoys
used for model validation, and at which projections are given.
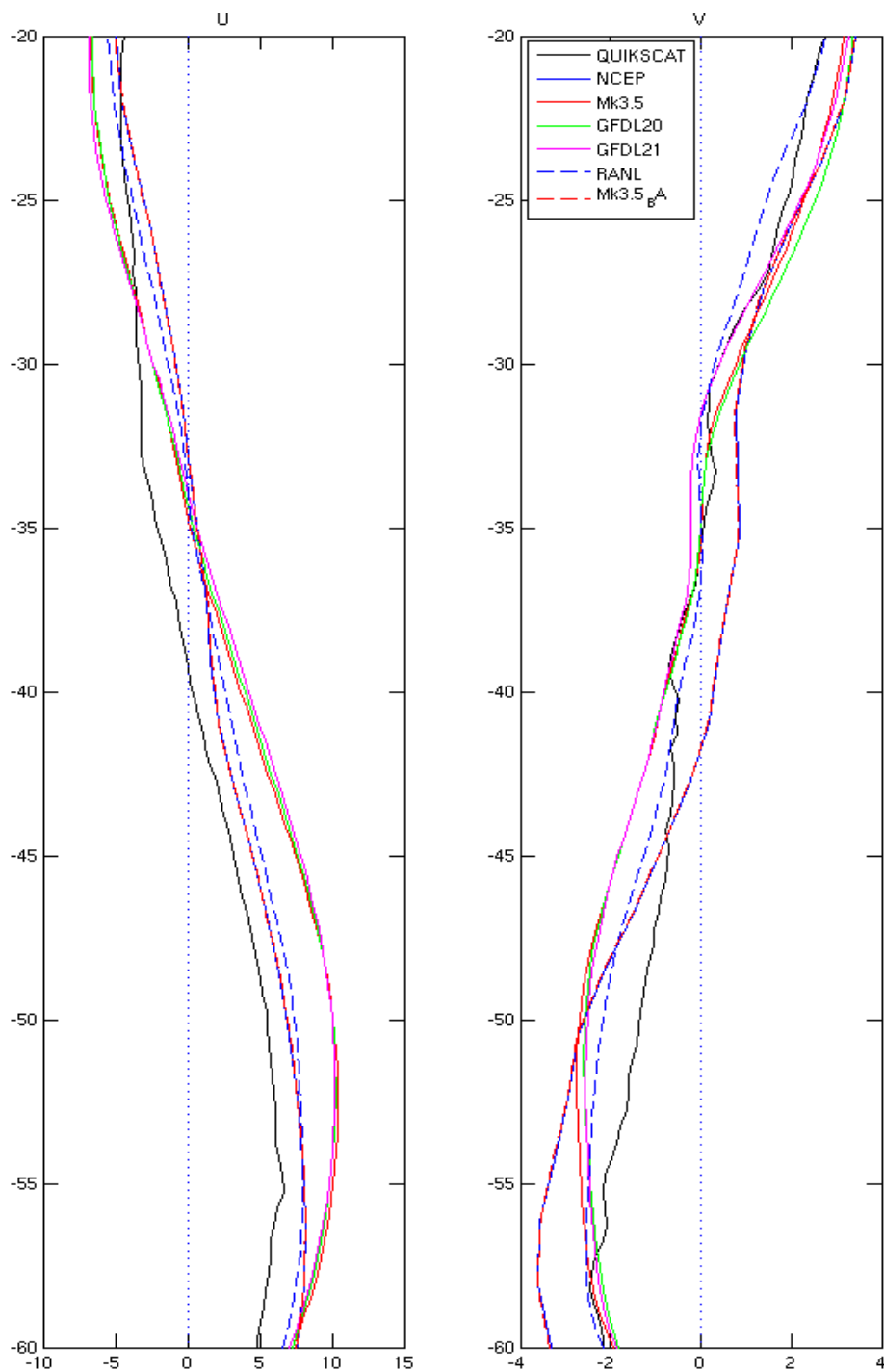
Figure 3. 20-yr (1981-2000) mean surface wind vector components (u –
eastwards, and v – northwards, units ms^{-1}) from the CCAM models along the
155°E meridian. Overlaid are mean winds from the NR A and the 1999-2007
mean QuikSCAT wind components. Note that the Mk3.5-BA winds (dashed
red line) overlays the NRA (solid blue line) winds almost exactly.
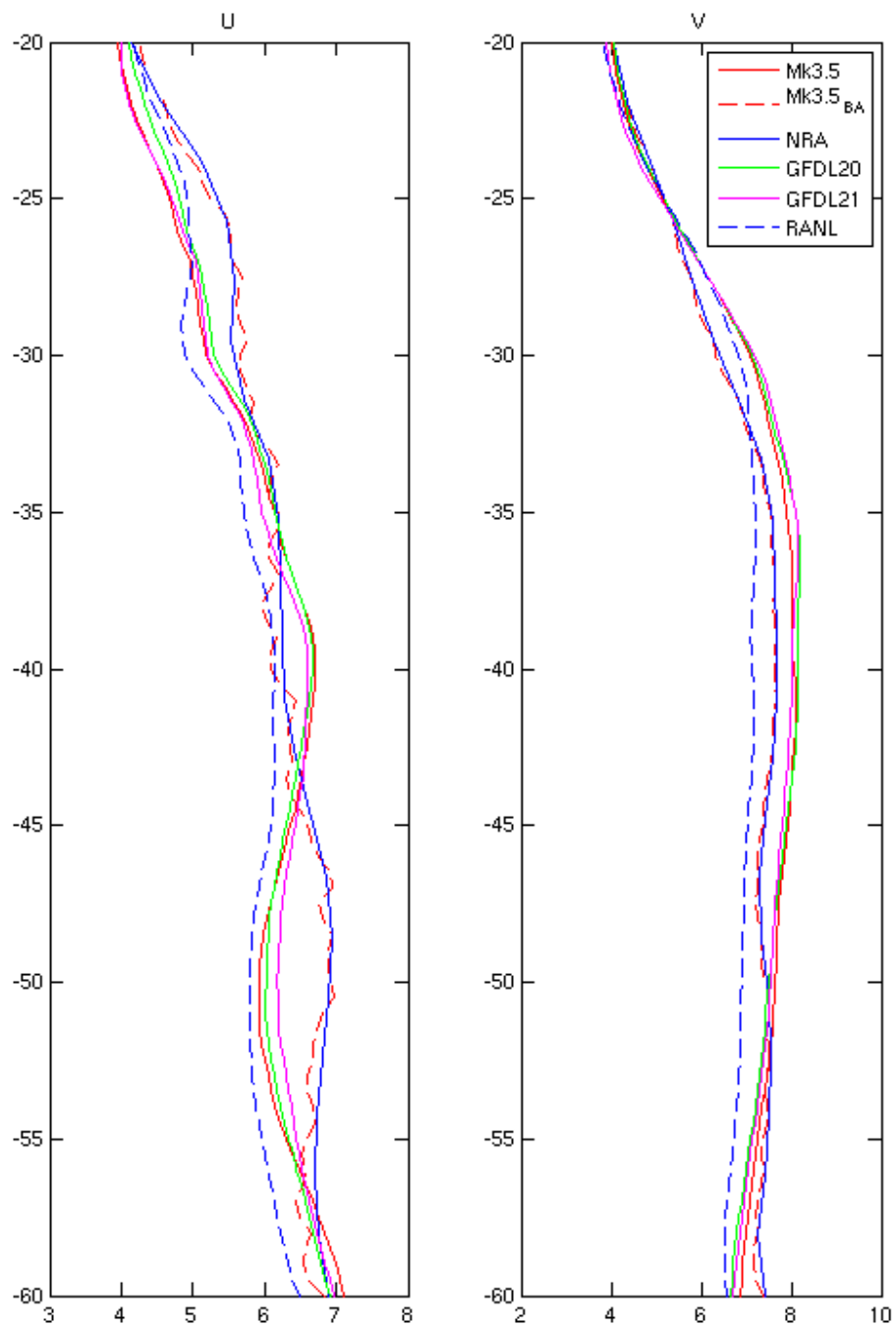
Figure 4. 20-yr (1981-2000) Standard Deviation (ms^{-1}) of the CCAM surface wind vector components (u – eastwards, v – northwards) along the 155°E meridian. Overlaid is the standard deviation of the NRA surface winds.
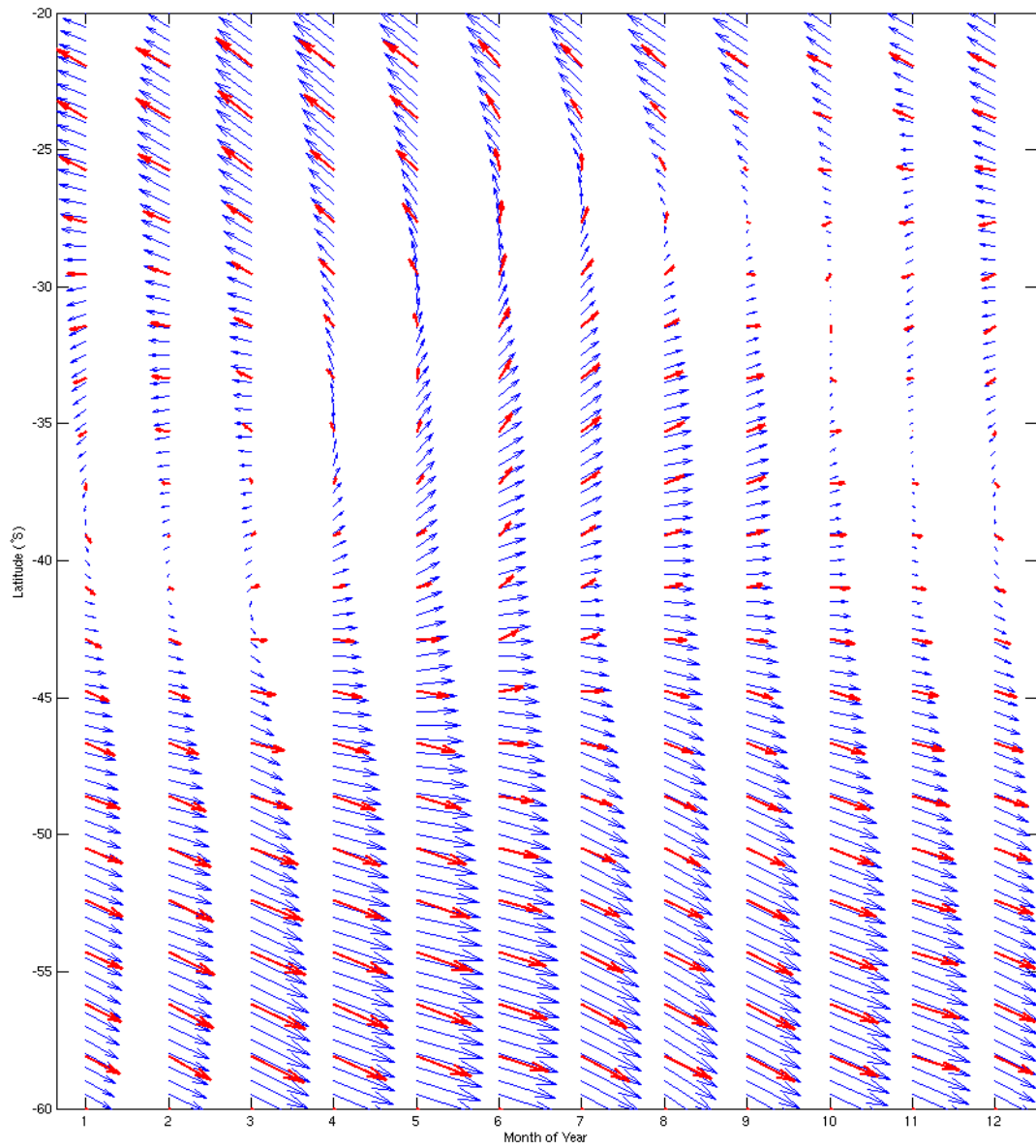
Figure 5. 20-yr (1981-2000) monthly mean winds along the 155°E meridian from CCAM CSIRO Mk3.5-BA (blue), and NRA (red).
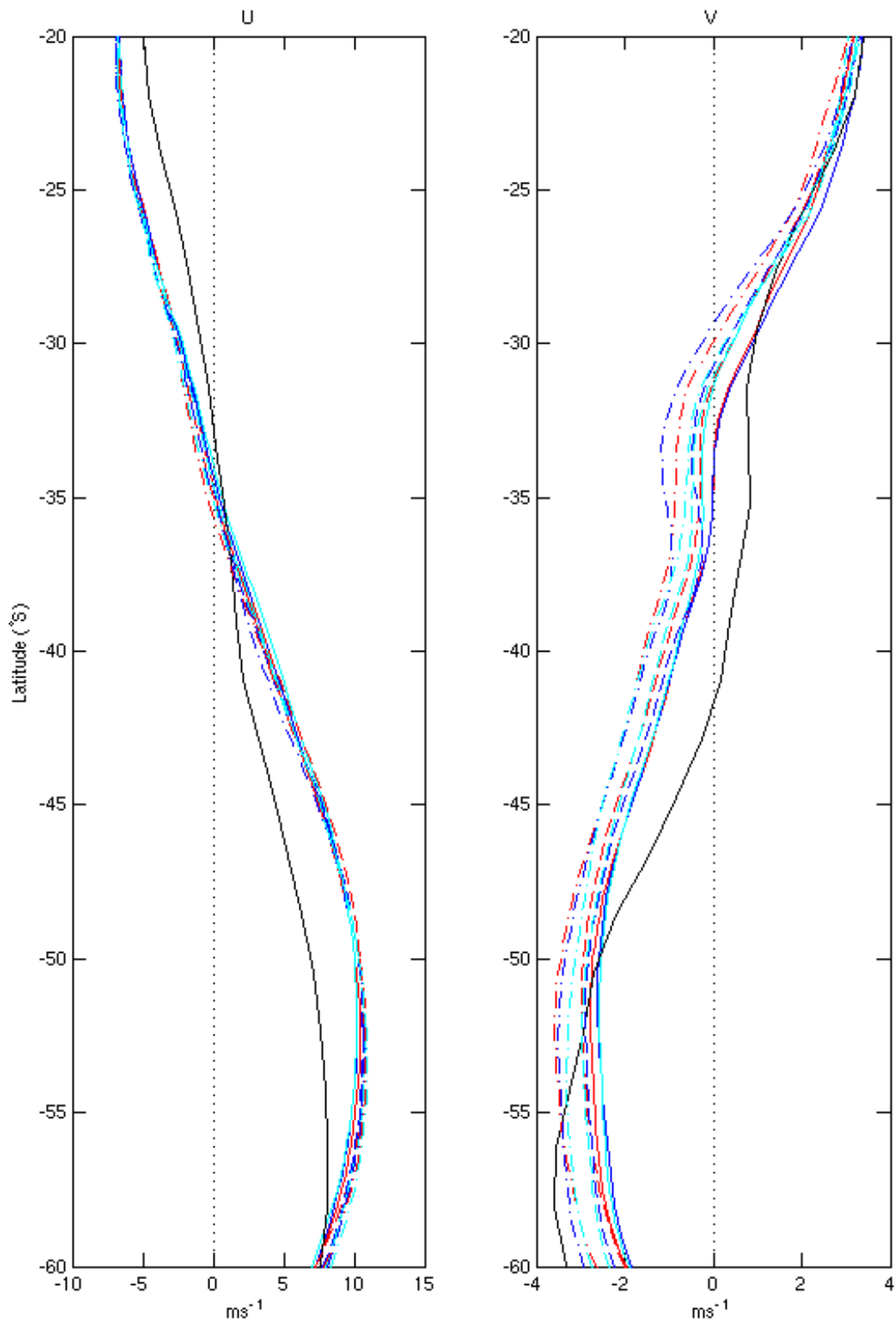
Figure 6. Multi-model ensembles of projected surface wind components along the 155°E meridian. Black line represents present d ay NRA climate. Red lines represent CCAM Mk3.5 runs, Dark blue lines represent CCAM GFDLcm2.0 runs, and light blue lines represent CCAM GFDLcm2.1 runs. Solid lines represent present climate mean (1981-2000), dashed lines represent mid-century mean (2031-2050), dash-dot lines represent end of century mean (2081-2100).
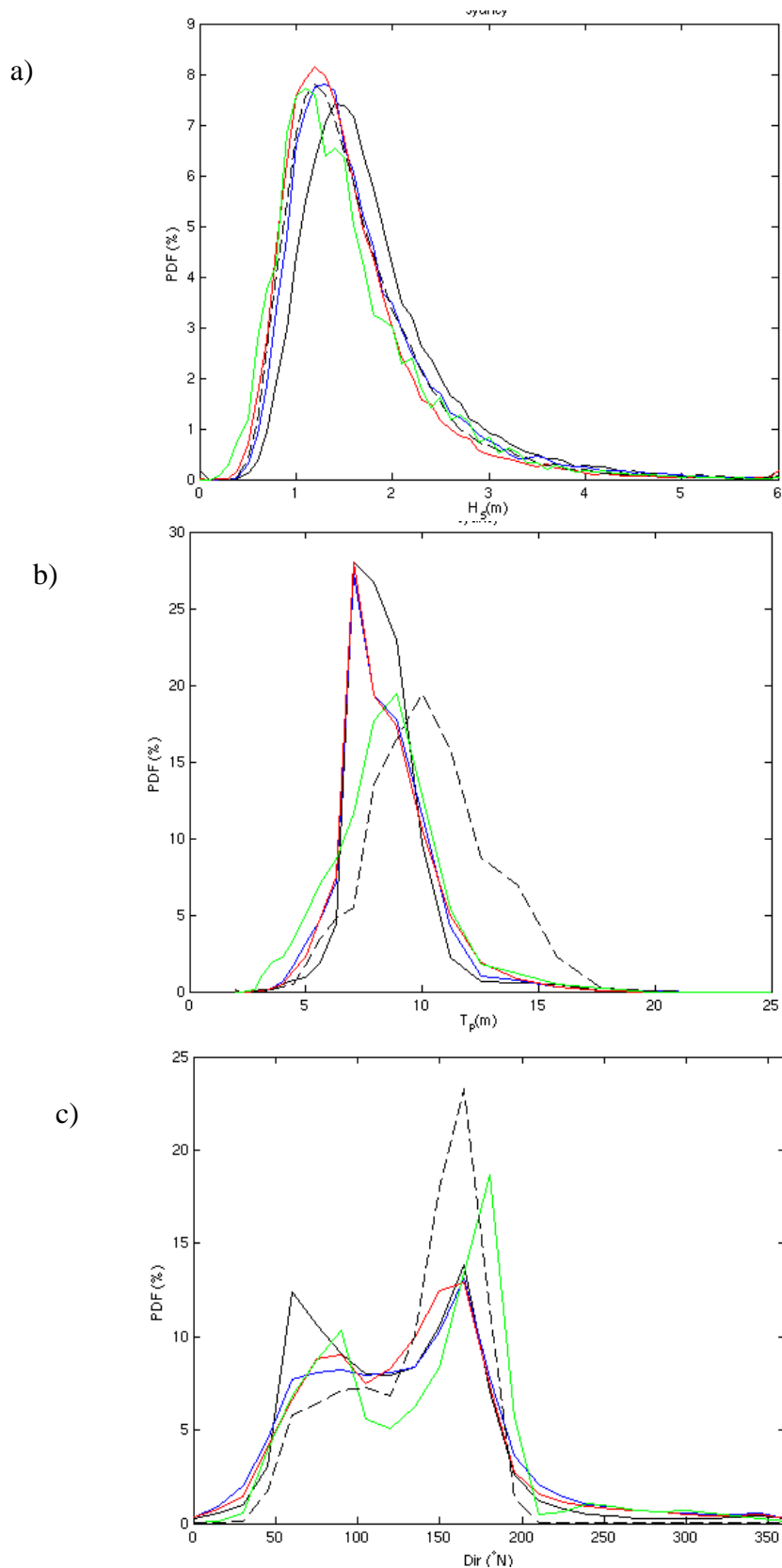
Figure 7. Integrated distributions of a) Significant Wave Height; b) Peak Wave Period; c) Peak wave Direction under present climate conditions at the Sydney waverider buoy site. Dotted black line – buoy data. Black line – CCAM Mk3.5. Blue line – CCAM Mk3.5-BA. Red line – NRA. Green line – NWW3.
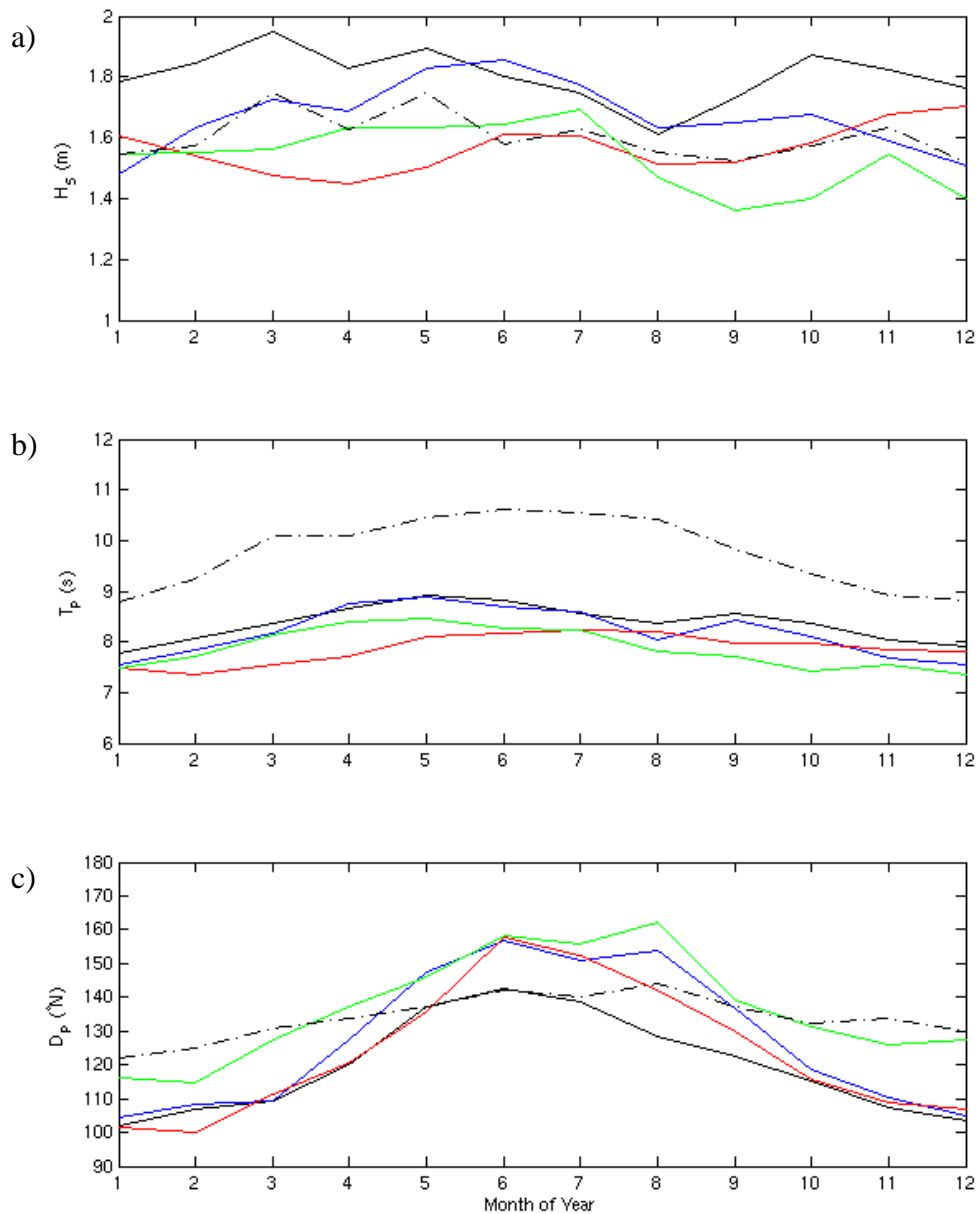
Figure 8. Annual cycle of mean Integrated wave parameters under present climate conditions at the location of the Sydney waverider buoy for a) Significant Wave Height; b) Peak Wave Period; c) Peak wave Direction. Dotted black line – buoy data. Black line – CCAM Mk3.5. Blue line – CCAM Mk3.5-BA. Red line – NRA. Green line – NWW3.
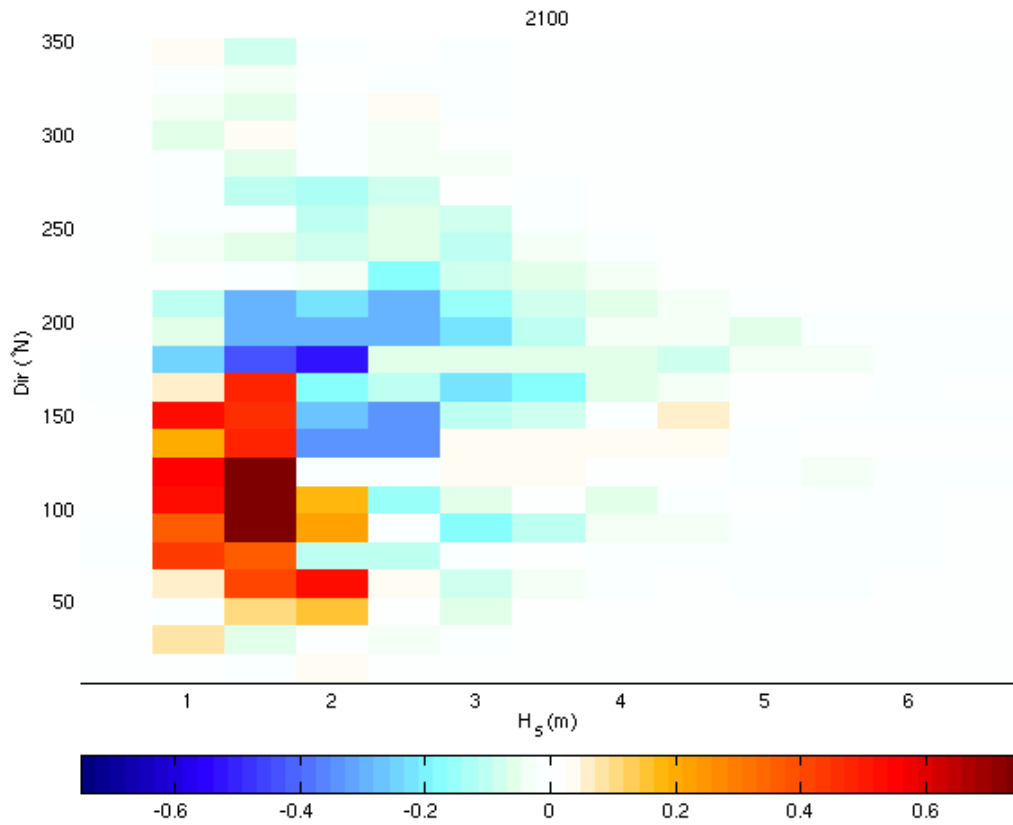
Figure 9. Difference between 2081-2100 and 1981-2000 Hs vs Dp bivariate distribution. Units are change in percentages.
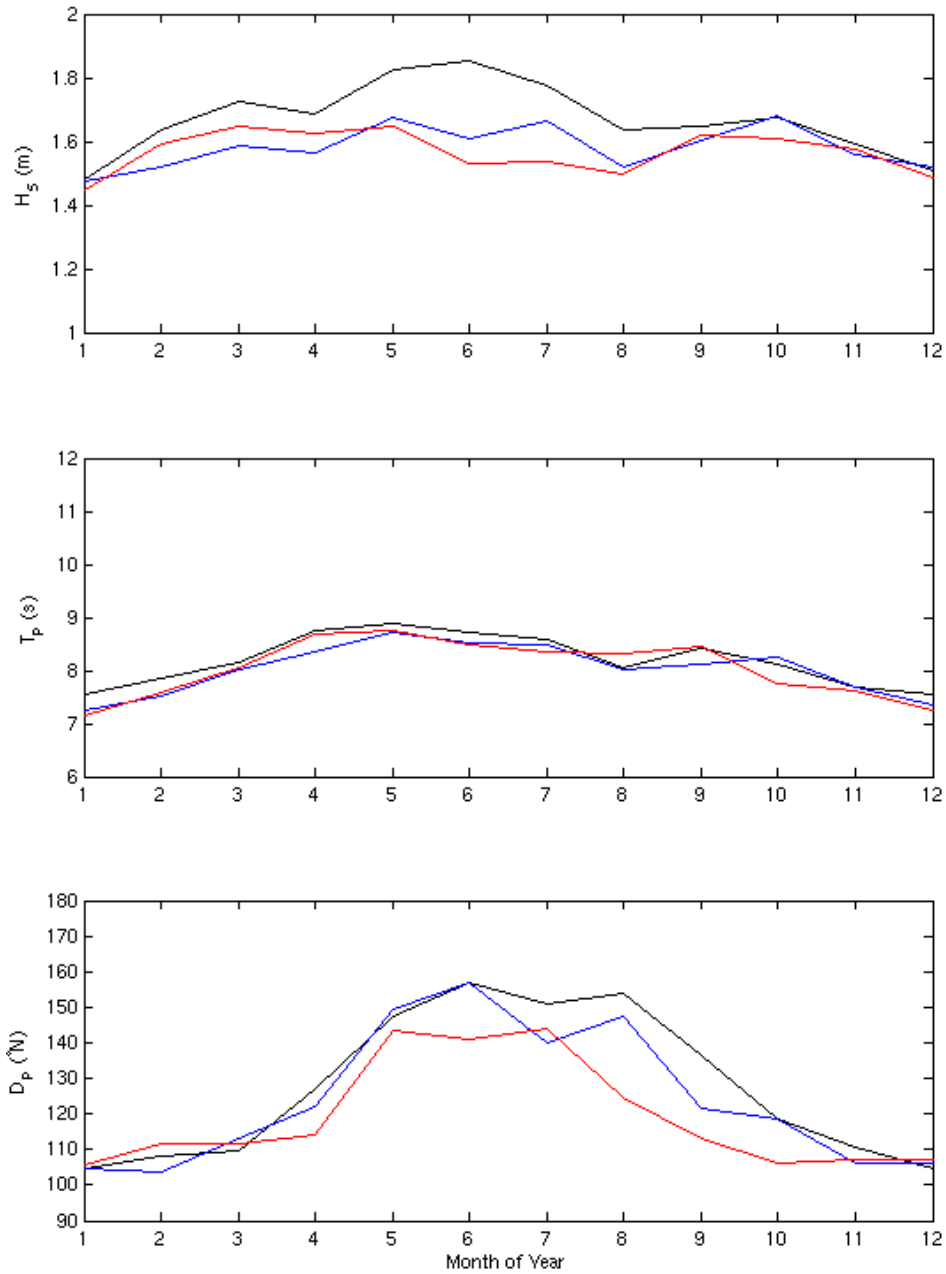
Figure 10. Monthly mean a) Significant Wave Height; b) Peak Wave Period; c) Peak wave Direction at the location of the Sydney waverider buoy derived from the SRES A2, CCAM Mk3.5-BA simulation. Black line – 1981-2000. Blue line – 2031-2050. Red line – 2081-2100.